Tectonics

Supporting Information for

Manifestations of syn-eruptive fluid circulations on carbonate veins, Central Anatolian Volcanic Province

Volkan Karabacak (1), Halim Mutlu (2), Kıymet Deniz (2)

(1) Department of Geological Engineering, Eskisehir Osmangazi University, Turkey (karabacak@ogu.edu.tr)

(2) Department of Geological Engineering, Ankara University, Turkey

Contents of this file

Introduction

This information includes supplementary figures and tables for sampling sites, results of sample analyses, and volcanic eruption records.

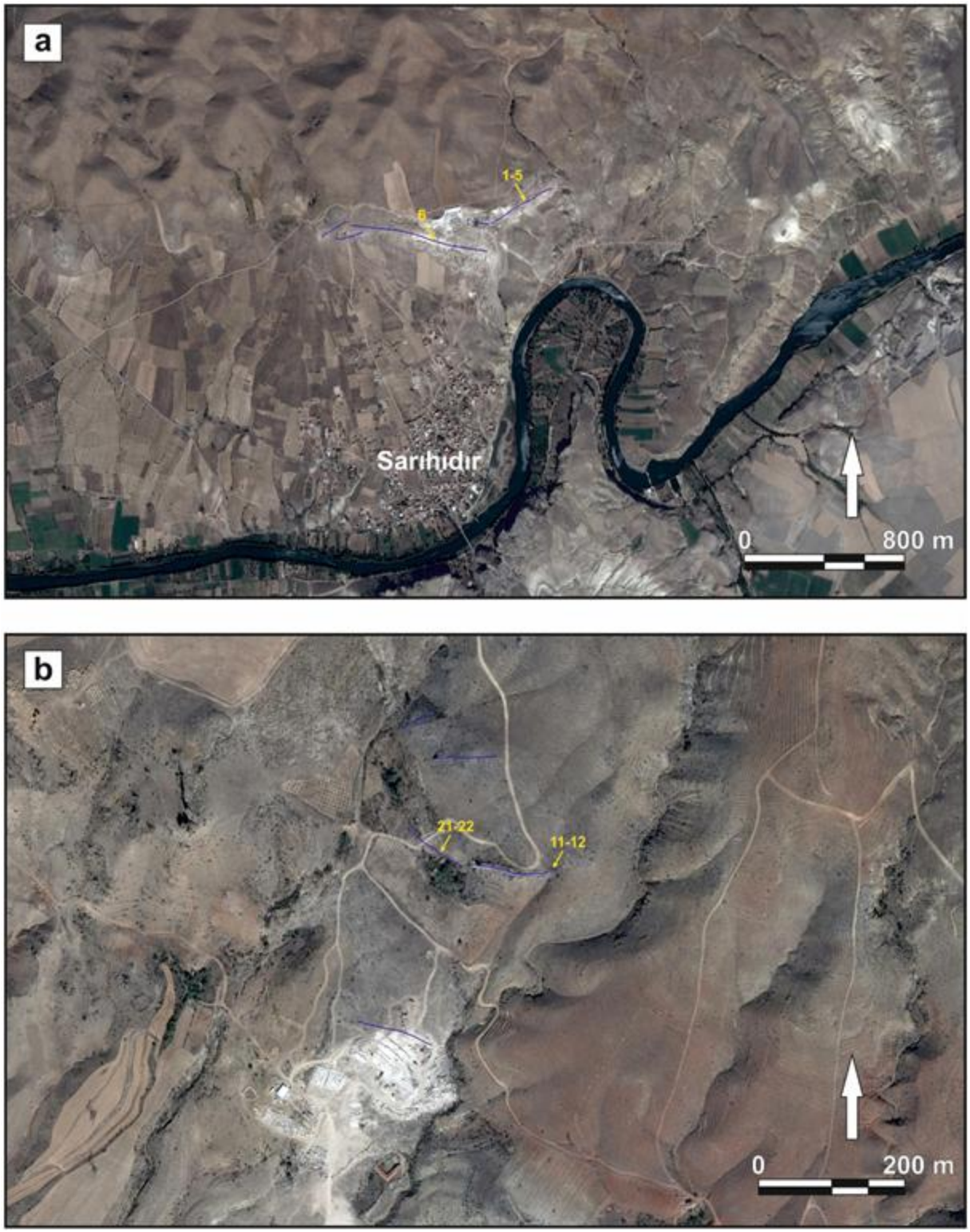

Figure S1. Satellite views of the carbonate veins and sampling locations (taken from Google Earth). a. Sarıhıdır site, b. Balkaya site.

Figure S2. Field views of the sampling location L1, Sarıhıdır. **a.** Well-protected morphology of the fissure ridge. **b.** Carbonate vein along the fissure ridge and **c.** collected samples.

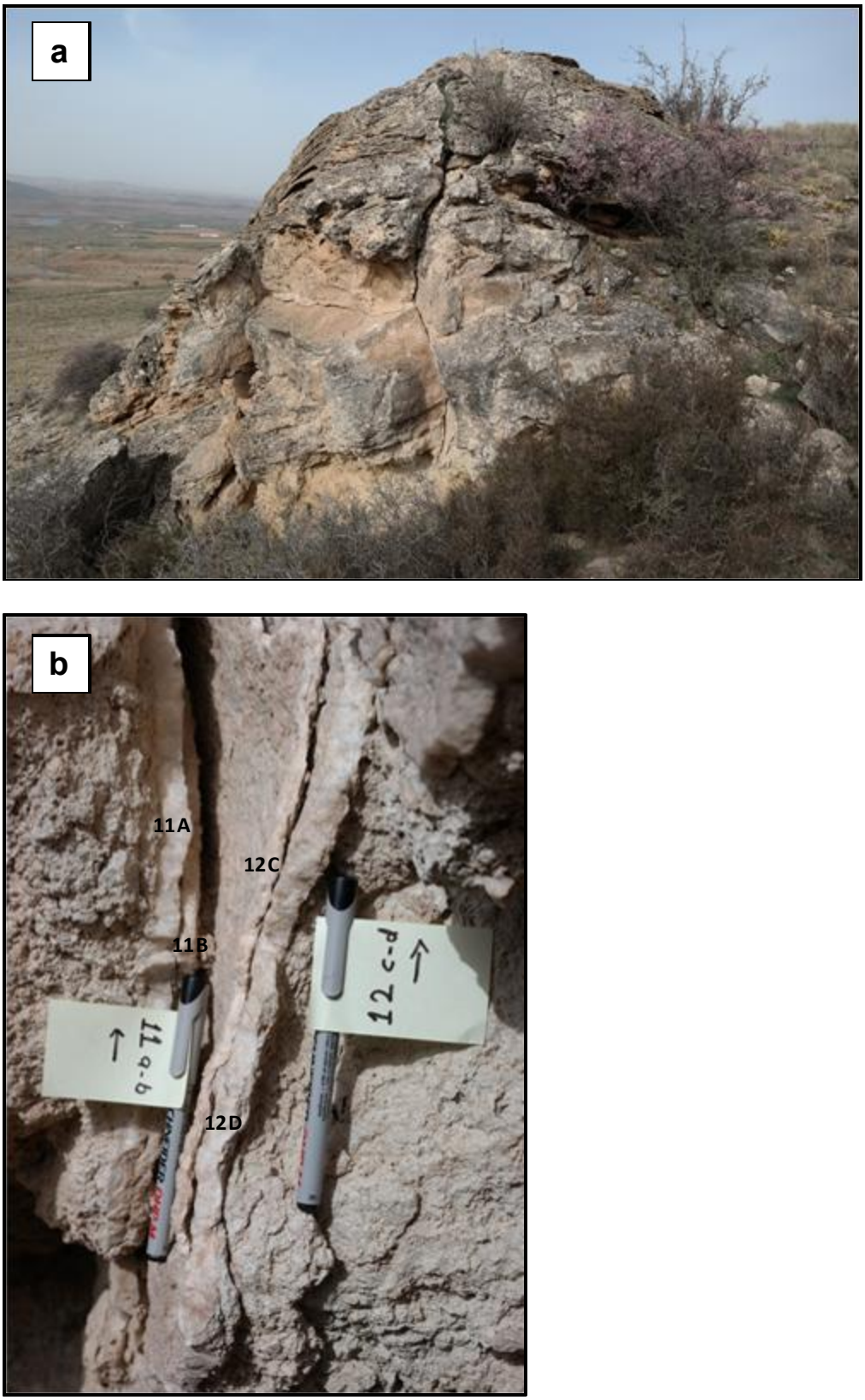

Figure S3. Field views of the sampling location L3, Balkaya. **a.** Well-protected morphology of the fissure ridge. **b.** Carbonate vein along the fissure ridge and collected samples.

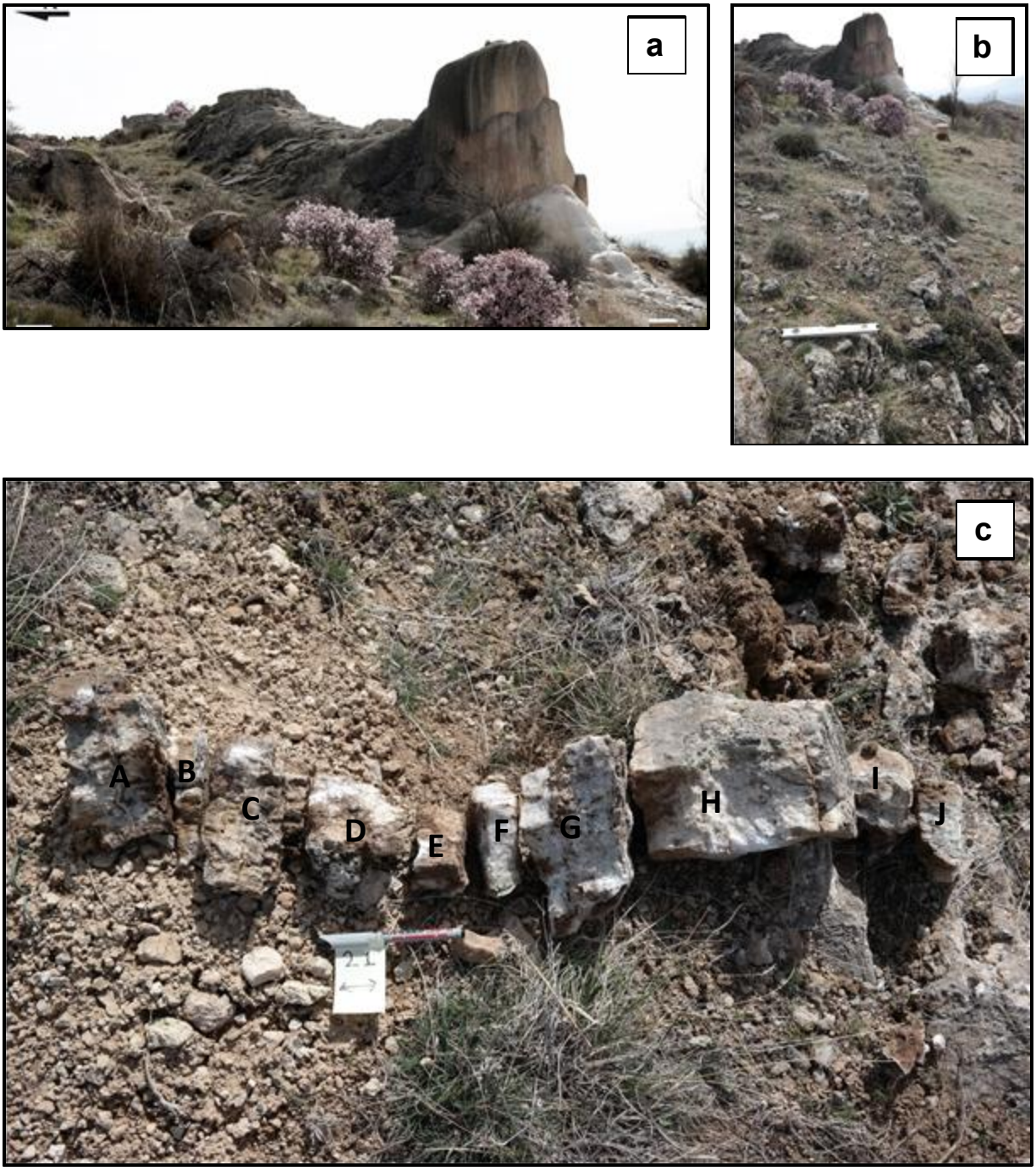

Figure S4. Field views of the sampling location L4, Balkaya. **a.** Well-protected morphology of the fissure ridge. **b.** Carbonate vein along the fissure ridge and **c.** collected samples.

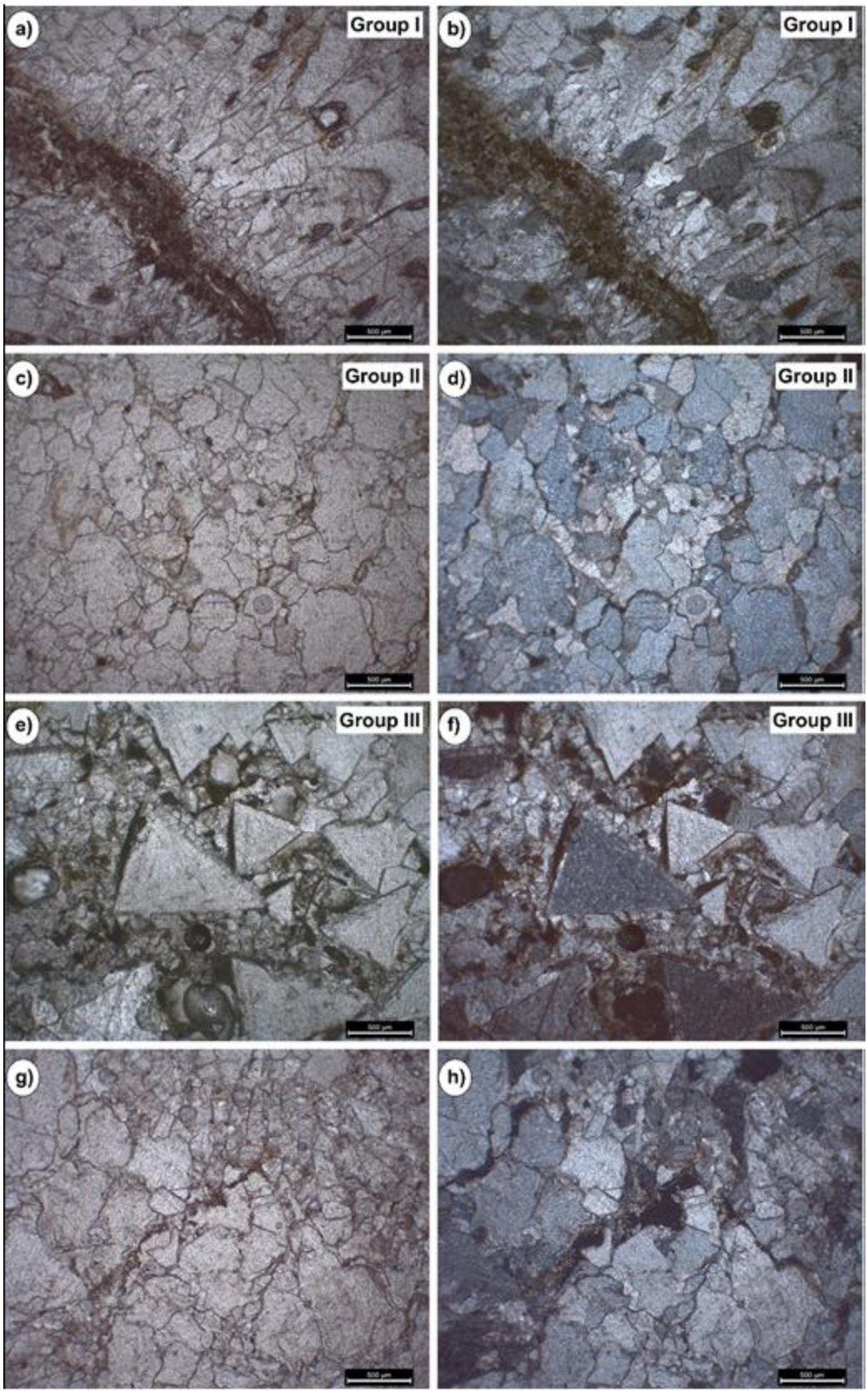

Figure S5. Representative thin section photos of the Balkaya samples. Photos at the right side are cross-polarized and those at the left are plane-polarized. a) and b) idiomorph, coarse crystalline, needle-shaped calcite minerals in sample A2; c) and d) mosaic texture in sample J1 showing various

sized xenomorphic calcites; e) and f) flow and granular textures with shelter porosity in sample H5; g) and h) fine crystalline granular texture with shelter and fenestral porosity in sample J1.

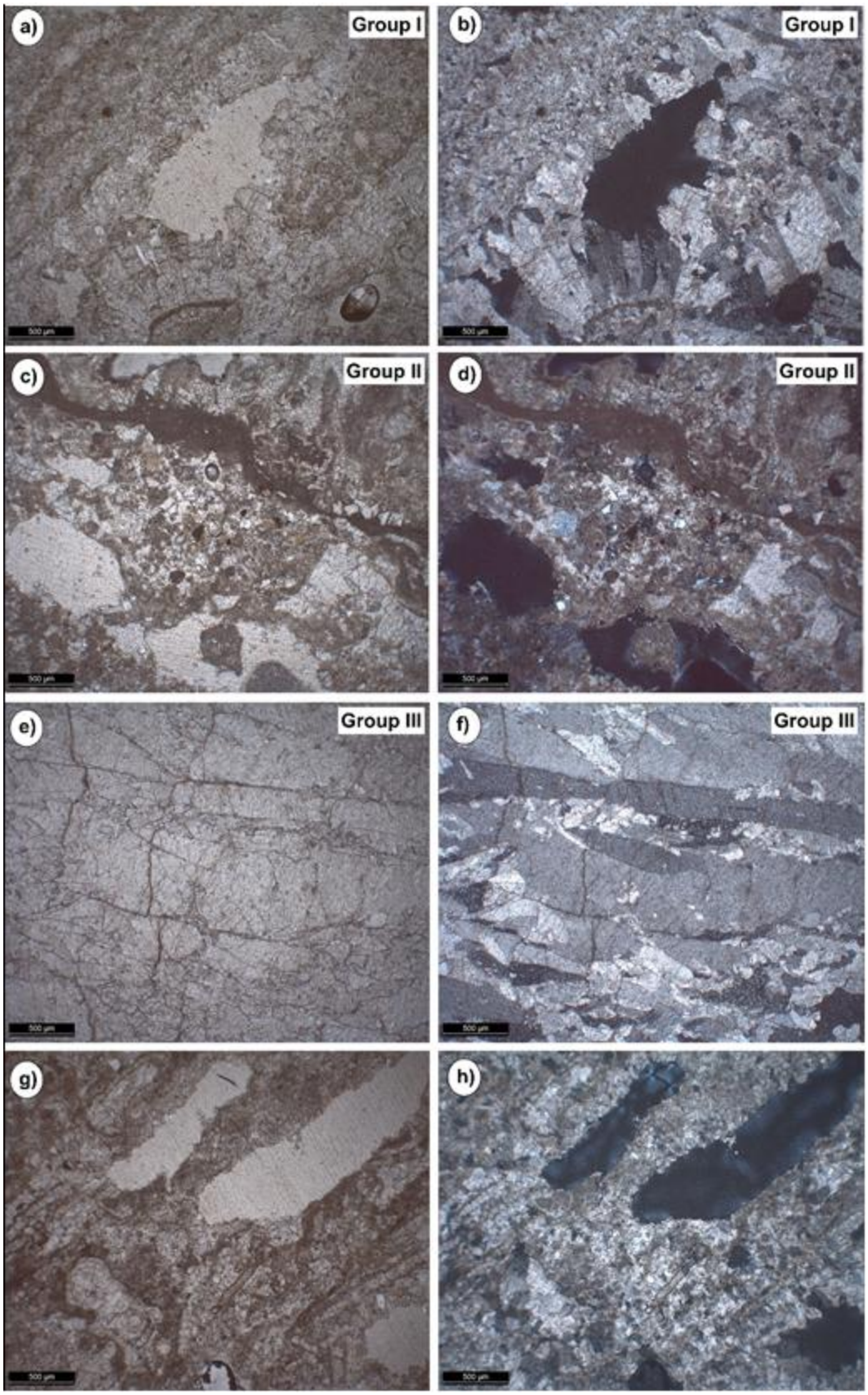

Figure S6. Representative thin section photos of the Sarıhıdır samples. Photos at the right side are cross-polarized and those at the left are plane-polarized. a) and b) fine to coarse crystalline calcite with rare quartz, pyroxene, epidote and clay minerals in sample 01; c) and d) finely crystalline granular texture and shelter type porosity in sample 03; e) and f) very finely banded and well

developed flow texture with shelter and fenestral type porosity in sample 04; g) and h) clay minerals in the carbonate bands of sample 01.

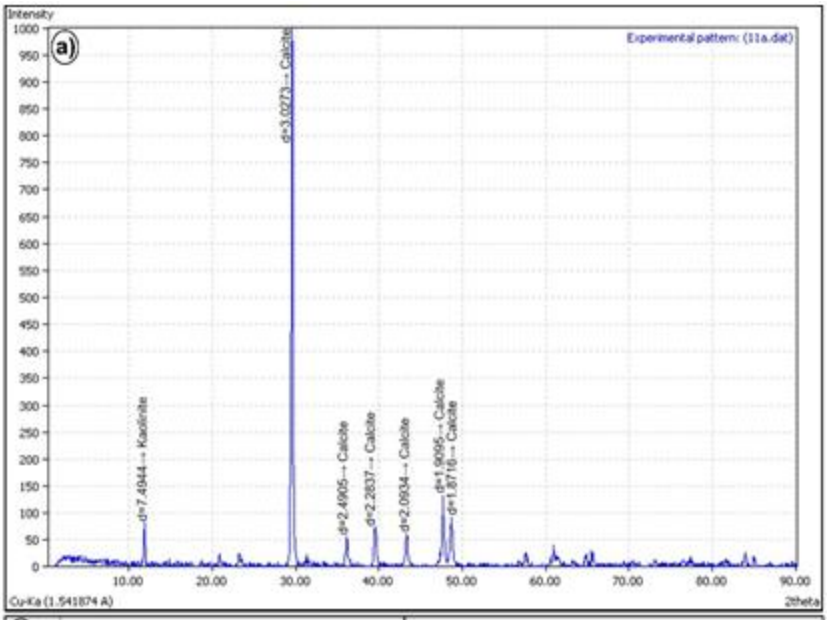

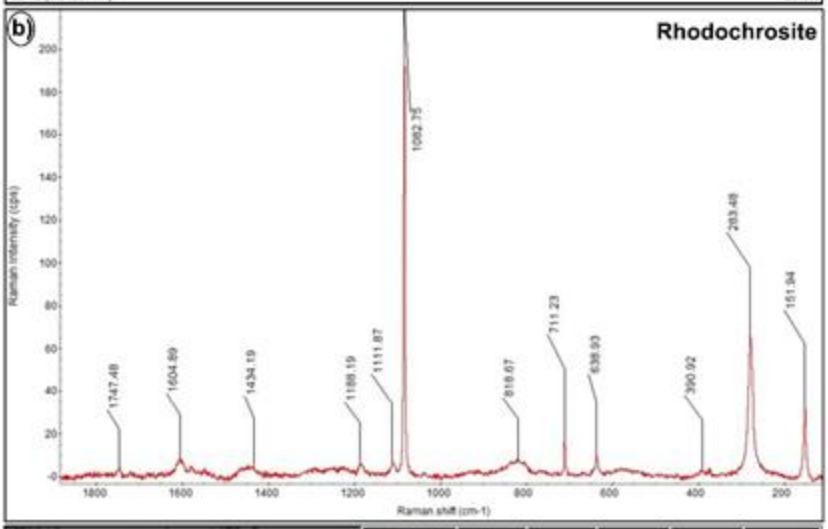

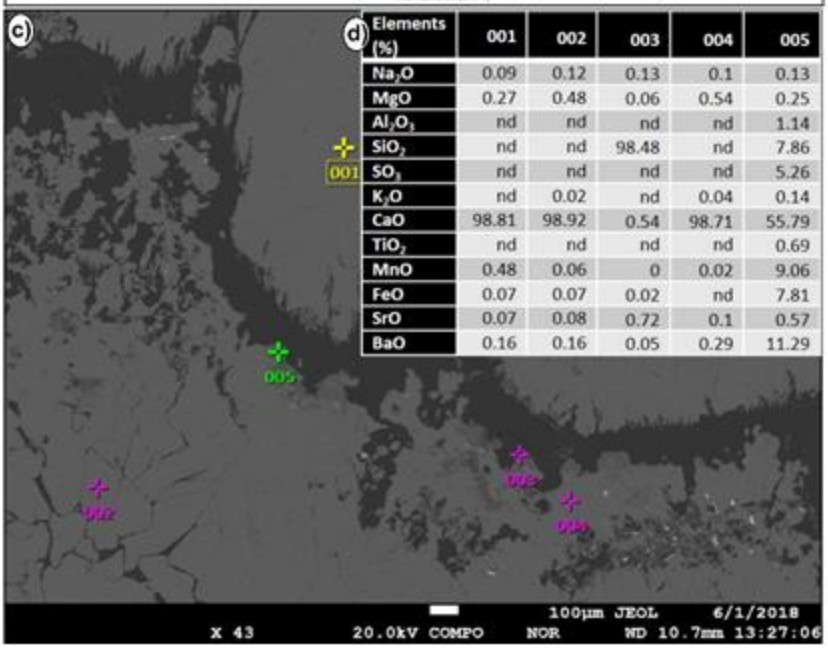

d)

Elements (%)	001	002	003	004	005
Na_2O	0.09	0.12	0.13	0.1	0.13
MgO	0.27	0.48	0.06	0.54	0.25
Al_2O_3	nd	nd	nd	nd	1.14
SiO_2	nd	nd	98.48	nd	7.86
SO_3	nd	nd	nd	nd	5.26
K_2O	nd	0.02	nd	0.04	0.14
CaO	98.81	98.92	0.54	98.71	55.79
TiO_2	nd	nd	nd	nd	0.69
MnO	0.48	0.06	0	0.02	9.06
FeO	0.07	0.07	0.02	nd	7.81
SrO	0.07	0.08	0.72	0.1	0.57
BaO	0.16	0.16	0.05	0.29	11.29

Figure S7. Representative (a) XRD (sample 11A), (b) CRS (A-2) and (c-d) EPMA (A-1) studies of samples from Balkaya site.

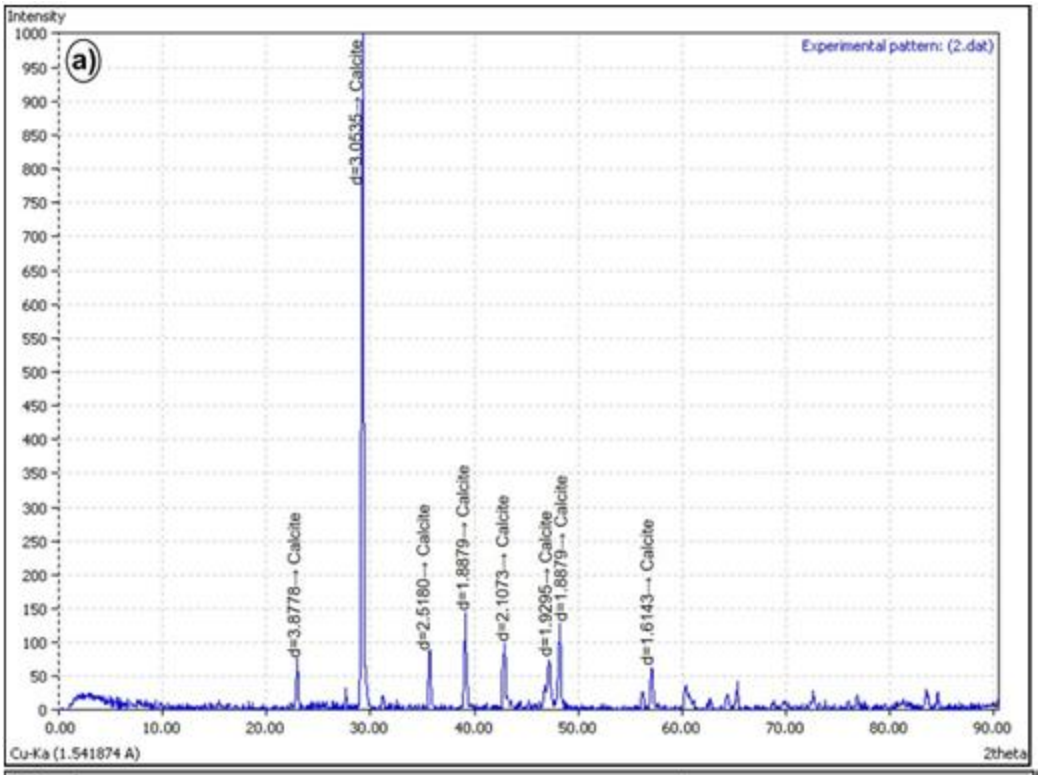

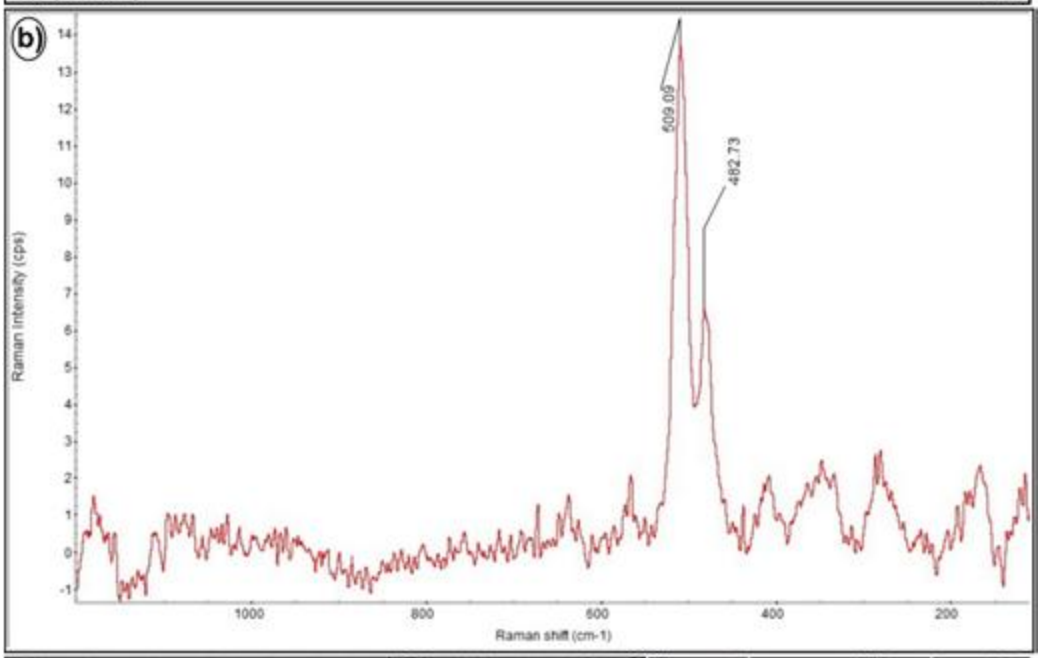

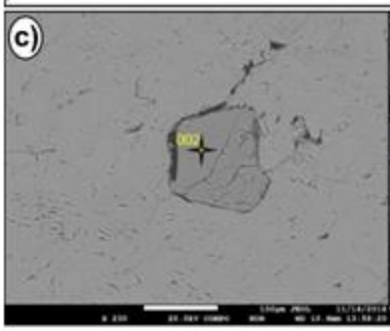

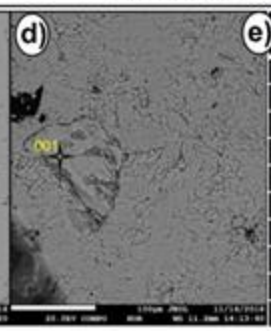

e)

Elements (%)	001 (Pyroxene)	002 (Epidote)
Na_2O	0.17	nd
SiO_2	52.35	57.91
MgO	15.67	0.01
Al_2O_3	3.11	27.81
MnO	0.15	0.05
K_2O	0.01	0.34
FeO	5.01	0.15
TiO_2	0.23	0.00
CaO	22.79	9.19
Total	100.16	95.46

Figure S8. Representative (a) XRD (sample 02), (b) CRS (sample 06-3) and (c-e) EPMA (sample 01) studies of samples from Sarıhıdır site.

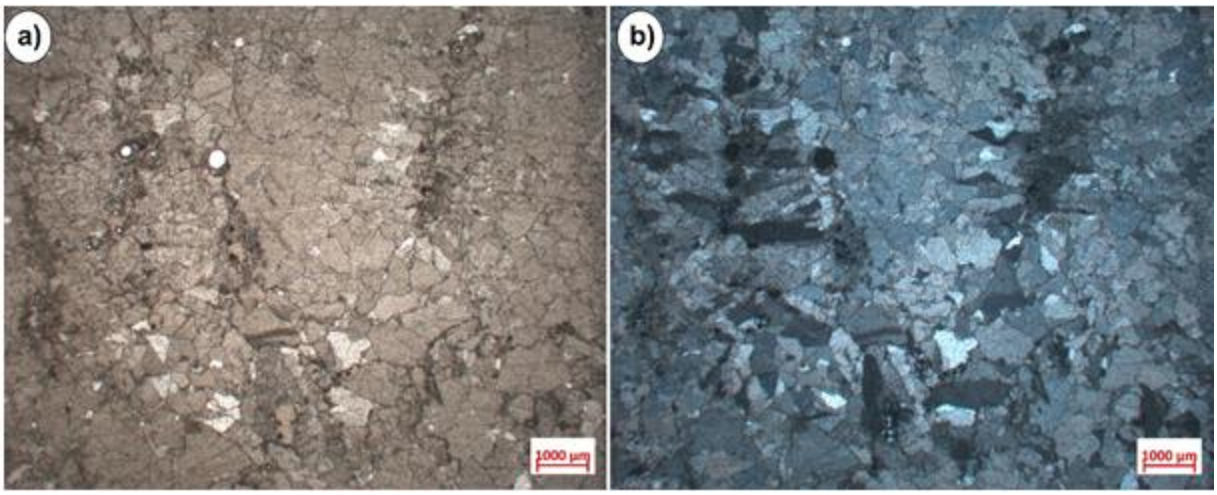

Figure S9. Thin section images of the Balkaya sample D1, which is dated at 130 ka; a) plane-polarized, b) cross-polarized.

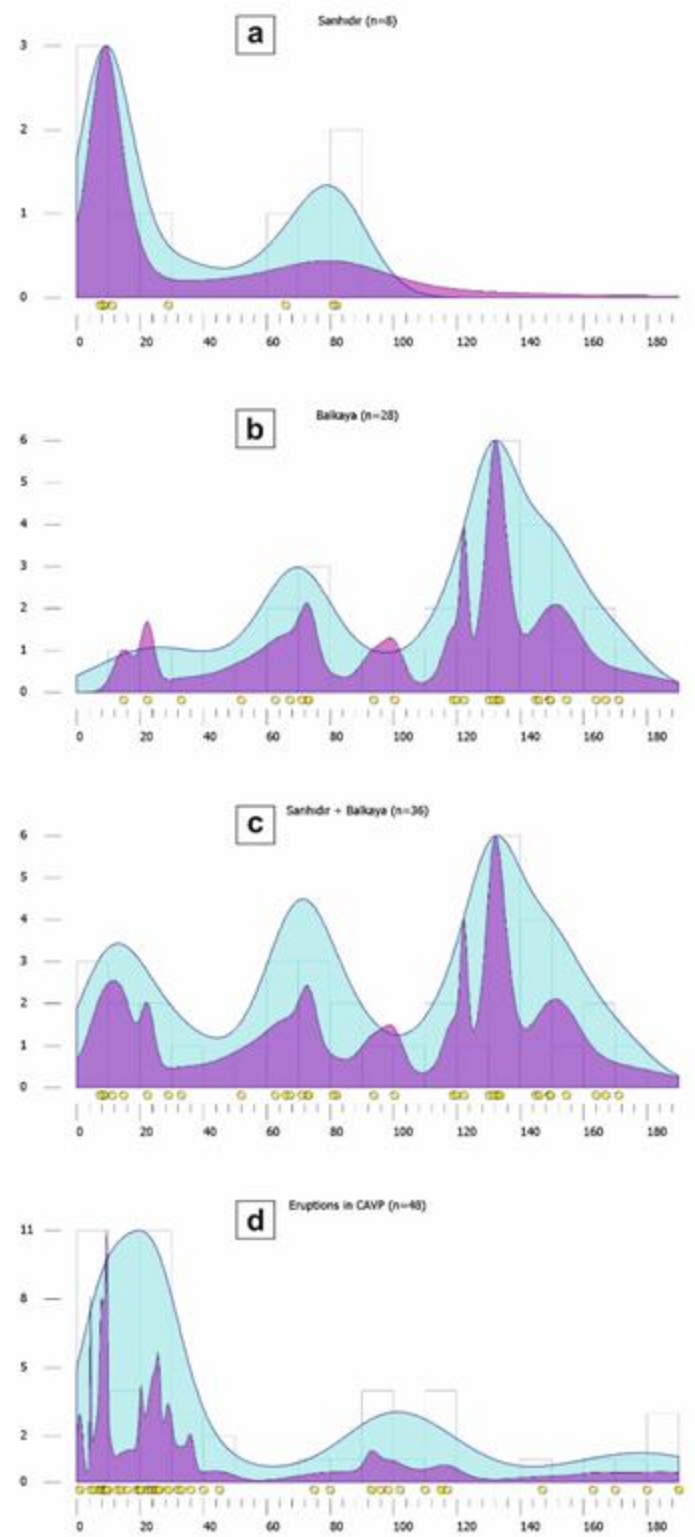

Figure S10. Relative probability curves of the U-series ages of carbonate samples and the previously dated paleo-eruptions. **a.** Sarıhıdır carbonate veins, **b.** Balkaya carbonate veins, **c.** the results of all carbonate samples, **d.** paleo-eruption records in literatures (Table S1) (purple plot: Probability density, light blue plot: Kernel density, rectangles: histograms of the samples). Note that x and y axes represent dating results in ka BP and number of samples respectively.

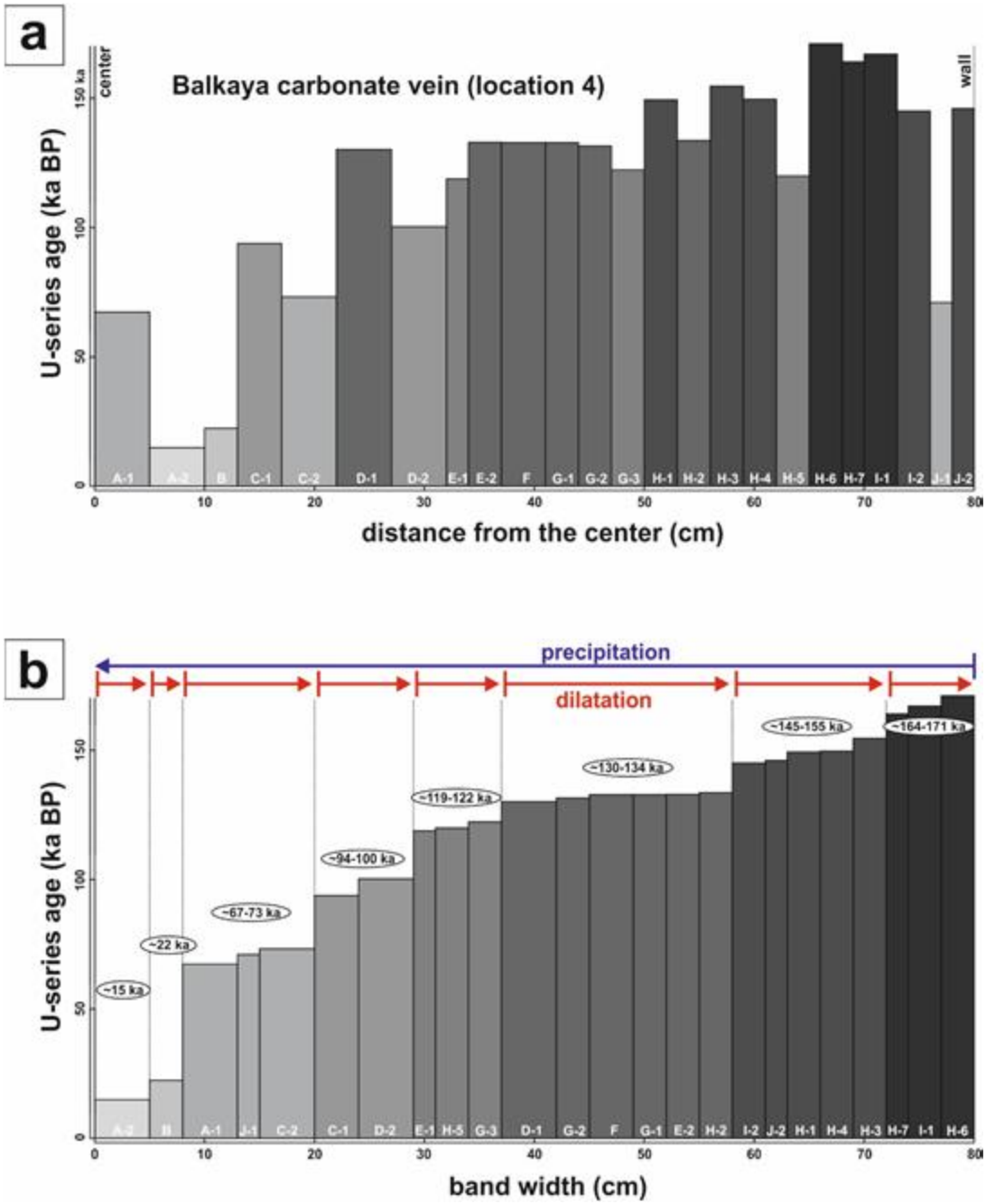

Figure S11. a. The U-series ages distribution of carbonate bands with respect to distance from the vein center to the wall on the L4-vein in Balkaya. Note that carbonate vein presents a continuous precipitation record. **b.** The graph is ordered as the coeval bands (U-series age vs. the band widths). Note that the vein has at least 8 rapid dilatation periods.

Table S1. Volcanic events dated in the last 190 ka around the study area.

	eruption date (ka BP)	eruption center	evidence	reference
1.	<1	Erciyes	basaltic lava (east of Hocalılar) (K-Ar)	Doğan-Külahcı, 2015
2.	<1	Erciyes	cinder cone lava-flow (south of Hacılar) (K-Ar)	Doğan-Külahcı, 2015
3.	4,4±0,2	Acıgöl	sediment cores in the late Pleistocene Eski Acıgöl maar, Tephra layer T17 (radiocarbon)	Kuzucuoglu et al., 1998
4.	5,5	Acıgöl	sediment cores in the late Pleistocene Eski Acıgöl maar, Tephra layer T15 (radiocarbon)	Kuzucuoglu et al., 1998
5.	8,2	Acıgöl	sediment cores in the late Pleistocene Eski Acıgöl maar, Tephra layer T13 (radiocarbon)	Kuzucuoglu et al., 1998
6.	7,2±0,9	Erciyes	lava-flow (Karagüllü) (cosmogenic ^{36}Cl)	Sarıkaya et al., 2017
7.	7,7±0,4	Erciyes	lava-flow (Perikartın) (cosmogenic ^{36}Cl)	Sarıkaya et al., 2017
8.	8,8±0,6	Erciyes	lava-flow (Dikkartın) (cosmogenic ^{36}Cl)	Sarıkaya et al., 2017
9.	8,9±0,6	Hasandağ	pumices collected from the summit of Big Hasandağ (U-Th/He method measured on zircon crystals)	Schmitt et al., 2014
10.	9,5±0,2	Erciyes	ash-flow (Erciyes) (^{14}C)	Sarıkaya et al., 2006
11.	9,8	Acıgöl	sediment cores in the late Pleistocene Eski Acıgöl maar, Tephra layer T10 (radiocarbon)	Kuzucuoglu et al., 1998
12.	13±5	Erciyes	cinder cone basalt (K-Ar)	Doğan-Külahcı, 2015
13.	14	Acıgöl	sediment cores in the late Pleistocene Eski Acıgöl maar, Tephra layer (radiocarbon)	Kuzucuoglu et al., 1998
14.	16	Acıgöl	Acıgöl maar (U-Th)	Roberts et al., 2001
15.	19	Acıgöl	acidic tephric layer with sphene and zircon (radiocarbon)	Kuzucuoglu et al., 1998
16.	20±6	Acıgöl	Guneydag dome (fission track age)	Bigazzi et al., 1993
17.	20,3±0,6	Acıgöl	Acıgöl maar, obsidian clast nearly aphyric (U-Th/He)	Schmitt et al., 2011
18.	22,3±1,1	Acıgöl	Karnıyarık, rhyolitic lava nearly aphyric (U-Th/He)	Schmitt et al., 2011
19.	23,2±3	Acıgöl	Kaleci, rhyolitic lava nearly aphyric (U-Th/He)	Schmitt et al., 2011
20.	23,8±0,9	Acıgöl	Güneydağ, rhyolitic lava nearly aphyric (U-Th/He)	Schmitt et al., 2011
21.	24,9±0,9	Acıgöl	Korudağ, rhyolitic lava nearly aphyric (U-Th/He)	Schmitt et al., 2011
22.	25±8	Erciyes	cinder cone lava-flow (Avşar Vilage) (K-Ar)	Doğan-Külahcı, 2015
23.	25,9±0,6	Acıgöl	Tepeköy, rhyolitic lava nearly aphyric (U-Th/He)	Schmitt et al., 2011
24.	26±1,5	Acıgöl	Kuzey, rhyolitic lava nearly aphyric (U-Th/He)	Schmitt et al., 2011
25.	28,9±1,5	Hasandağ	pumices collected from the flank of the volcano (U-Th/He method measured on zircon crystals)	Schmitt et al., 2014
26.	29±1	Hasandağ	from the summit (K-Ar)	Kuzucuoglu et al., 1998
27.	32±3	Acıgöl	south of Kocadağ (K-Ar)	Türkecan et al., 2004
28.	33±2	Hasandağ	from the summit (K-Ar)	Kuzucuoglu et al., 1998
29.	36,1±1,1	Erciyes	lava-flow (Çarık) (cosmogenic ^{36}Cl)	Sarıkaya et al., 2017
30.	40±7	Erciyes	fissure basalt (Karagüllü) (K-Ar)	Doğan-Külahcı, 2015
31.	45±5	Erciyes	basaltic lava (Sürtme Plateau) (K-Ar)	Doğan-Külahcı, 2015
32.	75	Acıgöl	Taşkesik, lava dome	Bigazzi et al., 1993
33.	80±10	Erciyes	augite-hypersthene andesite, lava-flow (Karigtepe) (K-Ar)	Notsu et al., 1995

34.	93±11	Erciyes	cinder cone lava-flow (north of Develi) (K-Ar)	Doğan-Külahcı, 2015
35.	93±2	Acıgöl	Boğazköy (obsidian)	Türkecan et al., 2004
36.	96,0±13,0	Acıgöl	basaltic lava (Karnıyarık Hill) (Ar-Ar)	Doğan, 2011
37.	98,4±3,6	Erciyes	lava-flow (Çarık) (kosmogenic ^{36}Cl)	Sarıkaya et al., 2017
38.	102±7	Erciyes	cinder cone basalt (south of Erciyes) (K-Ar)	Doğan-Külahcı, 2015
39.	110±40	Acıgöl	upper Acıgöl tuff (ITPFT isothermal plateau fission track age)	Druitt et al., 1995
40.	115±7	Erciyes	basaltic lava (Şeyhşaban) (K-Ar)	Doğan-Külahcı, 2015
41.	115±20	Erciyes	dacite-flow (Dikkartın) (Ar-Ar)	Ercan et al., 1994
42.	117±4	Acıgöl	Alacasar, rhyolitic pumice aphyric (U-Th/He)	Schmitt et al., 2011
43.	147±8	Acıgöl	Taşkesik, rhyolitic lava nearly aphyric (U-Th/He)	Schmitt et al., 2011
44.	163±7	Acıgöl	upper Acıgöl tuffs Boğazköy, rhyolitic pumice aphyric (U-Th/He)	Schmitt et al., 2011
45.	170±10	Erciyes	hypersthene andesite, lava-flow (south of Kayseri) (K-Ar)	Notsu et al., 1995
46.	180	Acıgöl	lower Acıgöl tuffs (ITPFT isothermal plateau fission track)	Druitt et al., 1995
47.	190±9	Acıgöl	Boğazköy, rhyolitic lava nearly aphyric (U-Th/He)	Schmitt et al., 2011
48.	190±11	Acıgöl	Kocadağ, rhyolitic lava weakly porphyritic (U-Th/He)	Schmitt et al., 2011

Table S2. General features of the sampling veins.

site	location	sample	band width (cm)	cordinates		strike/dip
SARIHIDIR	1	01	6	0667945E	4290662N	N50E/90
		02	2			
		03	4			
		04	4			
		05	3			
	2	06-1	3	0667666E	4290473N	N85W/90
		06-2	3			
		06-3	3			
BALKAYA	3	11A	1	0658004E	4290500N	N70E/78SE
		11B	0,5			
		12C	0,5			
		12D	1			
	4	A-1	5	0657826E	4290507N	N70W/90
		A-2	5			
		B	3			
		C-1	4			
		C-2	5			
		D-1	5			
		D-2	5			
		E-1	2			
		E-2	3			
		F	4			
		G-1	3			
		G-2	3			
		G-3	3			
		H-1	3			
		H-2	3			
		H-3	3			
		H-4	3			
		H-5	3			
		H-6	3			
		H-7	2			
		I-1	3			
		I-2	3			
		J-1	2			
		J-2	2			

Table S3. Mineralogical and petrographical properties of representative Balkaya and Sarıhıdır travertine samples.

site	group	sample	texture	mineralogy	mineral shape	crystal form	porosity type
BALKAYA	I	A-2	Banded, flow	Mainly calcite	Idiomorph	Needle-shaped	Burrowing
		C					
		E-1					
		F					
		H-6					
	II	A-1	Granular (Mosaic)	Mainly calcite	Xenomorph	Granular	Fenestral
		H-2					
		H-3					
		H-4					
		H-7					
		J-1					
	III	H-5	Granular, flow	Mainly calcite	Xenomorph		Shelter
	IV	G-3	Fine crystalline granular	Mainly calcite	Xenomorph	Granular	Shelter, Fenestral
		11B		Mainly calcite, quartz			
		B		Mainly calcite	Idiomorph	Needle-shaped	Fenestral
SARIHIDIR	I	01	Granular rarely banded (flow)	Mainly calcite, quartz, pyroxene, plagioclase, clay minerals	Idiomorph and xenomorph	Needle-shaped	Shelter
		06-3		Mainly calcite, quartz, epidote, clay, plagioclase		Needle-shaped, granular	
	II	03	Granular (Mosaic)	Mainly calcite, quartz, opaque mineral, feldspar	Xenomorph	Granular	Shelter
		05		Mainly calcite			
	III	02	Banded, flow	Mainly calcite, clay minerals	Idiomorph	Needle-shaped	Shelter
		06-1		Mainly calcite			Shelter
		06-2		Mainly calcite, quartz			Shelter, fenestral
		04		Mainly calcite			Fenestral

Table S4. Summary of MC-ICP-MS Uranium (U)-series age data.

site	location	sample	U (ppm)	±2s	^{232}Th (ppb)	±2s	(^{230}Th/^{232}Th)	±2s	(^{230}Th/^{238}U)	±2s	(^{234}U/^{238}U)	±2s	uncorr. age (ka)	±2s	corr. age (ka)	±2s
SARIHIDIR	1	01	0,02939	0,00005	71,19	0,21	0,996	0,005	0,7951	0,0038	1,2260	0,0026	109,0	1,0	29	50
		02	0,01044	0,00005	4,798	0,020	1,392	0,033	0,2109	0,0050	1,2833	0,0064	19,45	0,51	8,4	5,7
		03	0,01424	0,00004	7,725	0,026	1,517	0,021	0,2712	0,0038	1,4021	0,0034	23,20	0,36	11,3	6,0
		04	0,00843	0,00004	2,778	0,009	1,705	0,027	0,1851	0,0030	1,3189	0,0053	16,39	0,29	8,8	3,8
		05	0,03015	0,00005	23,334	0,060	1,120	0,010	0,2856	0,0025	1,3396	0,0027	25,88	0,26	7,5	9,8
	2	06-1	0,01079	0,00004	31,73	0,10	1,055	0,007	1,0219	0,0077	1,1987	0,0048	188,1	4,2	82	121
		06-2	0,00681	0,00005	16,043	0,069	1,187	0,010	0,9217	0,0093	1,2378	0,0071	138,9	3,2	66	39
		06-3	0,00721	0,00003	9,673	0,022	1,840	0,016	0,8138	0,0077	1,2012	0,0050	117,9	2,2	81	16
BALKAYA	3	11A	0,016727	0,000007	18,09	0,014	2,221	0,011	0,7917	0,0038	1,5649	0,0030	73,2	0,5	52,1	8,4
		11B	0,016056	0,000005	16,75	0,028	2,462	0,013	0,8464	0,0042	1,5262	0,0029	83,4	0,6	62,8	8,4
		12C	0,013963	0,000003	15,29	0,013	1,710	0,012	0,6171	0,0044	1,4857	0,0019	56,7	0,5	33	10
		12D	0,014266	0,000005	18,82	0,025	2,178	0,012	0,9473	0,0052	1,5161	0,0030	99,6	0,9	73	13
	4	A-1	0,025181	0,000009	13,89	0,014	3,660	0,020	0,6651	0,0036	1,2473	0,0021	80,6	0,7	67,3	5,6
		A-2	0,03204	0,00005	7,721	0,013	2,571	0,022	0,2042	0,0018	1,1506	0,0024	21,21	0,21	14,9	3,2
		B	0,017004	0,000013	2,81	0,003	4,696	0,037	0,2561	0,0020	1,1782	0,0021	26,6	0,2	22,4	2,1
		C-1	0,012462	0,000004	5,38	0,004	5,787	0,052	0,8232	0,0073	1,3040	0,0025	103,4	1,5	93,8	3,9
		C-2	0,03360	0,00005	9,583	0,020	7,239	0,053	0,6805	0,0049	1,2825	0,0031	79,70	0,87	73,2	2,6
		D-1	0,02988	0,00006	11,661	0,025	8,103	0,049	1,0423	0,0062	1,3857	0,0030	137,8	1,6	130,1	4,9
		D-2	0,008405	0,000005	3,06	0,004	7,287	0,046	0,8750	0,0054	1,3453	0,0032	107,9	1,2	100,3	3,2
		E-1	0,018412	0,000005	5,60	0,006	9,468	0,041	0,9485	0,0040	1,3368	0,0022	125,1	1,0	118,8	2,9
		E-2	0,018412	0,000004	3,78	0,004	15,083	0,084	1,0193	0,0056	1,3631	0,0022	137,0	1,5	132,9	2,7
		F	0,037433	0,000010	12,56	0,012	9,199	0,034	1,0175	0,0036	1,3489	0,0022	139,6	1,0	132,8	3,9
		G-1	0,008494	0,000003	2,39	0,002	11,037	0,061	1,0238	0,0056	1,3616	0,0028	138,4	1,5	132,8	3,5
		G-2	0,01292	0,00004	0,900	0,002	45,52	0,32	1,0451	0,0078	1,4143	0,0042	132,8	2,0	131,5	2,1
		G-3	0,021214	0,000007	0,2534	0,0003	242,3	1,3	0,9539	0,0049	1,3578	0,0020	122,6	1,1	122,3	1,1
		H-1	0,01237	0,00004	5,726	0,016	7,088	0,057	1,0817	0,0088	1,3436	0,0038	158,7	2,9	149,3	7,5
		H-2	0,00747	0,00003	1,707	0,005	13,49	0,11	1,0152	0,0090	1,3520	0,0043	138,1	2,5	133,6	3,5
		H-3	0,011022	0,000004	3,75	0,003	10,088	0,055	1,1319	0,0062	1,3901	0,0026	161,0	1,9	154,6	6,0
		H-4	0,02601	0,00006	8,926	0,022	9,966	0,048	1,1272	0,0054	1,4032	0,0030	156,1	1,7	149,6	5,8
		H-5	0,006597	0,000002	4,81	0,004	4,179	0,027	1,0052	0,0065	1,3541	0,0025	135,3	1,7	119,9	8,7
		H-6	0,02863	0,00005	19,761	0,059	5,321	0,042	1,2105	0,0091	1,3980	0,0033	183,8	3,4	171	18
		H-7	0,009489	0,000004	9,53	0,009	3,550	0,018	1,1754	0,0059	1,3611	0,0030	184,5	2,4	164	27
		I-1	0,019892	0,000008	12,15	0,012	5,915	0,028	1,1912	0,0055	1,3926	0,0028	179,1	2,1	167	15
		I-2	0,02425	0,00006	15,036	0,045	5,314	0,033	1,0861	0,0064	1,3526	0,0043	157,5	2,2	145	10
		J-1	0,015761	0,000005	19,36	0,024	1,878	0,008	0,7606	0,0032	1,2101	0,0025	104,0	0,8	71	15
		J-2	0,01572	0,00005	12,779	0,041	4,091	0,026	1,0961	0,0069	1,3456	0,0043	162,5	2,5	146	15

Table S5. Rare earth element and Ytriyum (Y) concentrations of the studied carbonate veins (ppb).

site	location	sample	La	Ce	Pr	Nd	Sm	Eu	Tb	Gd	Dy	Ho	Y	Er	Tm	Yb	Lu
SARIHIDIR	1	01	194	351	41	157	34	9	4	28	32	7	218	18	3	20	3
		03	41	93	9	42	8	3	1	10	11	2	80	7	1	8	1
		05	55	104	11	39	8	4	0	5	4	1	45	3	1	3	1
	2	06-1	105	187	23	88	19	13	4	24	36	9	345	38	7	54	9
		06-2	34	71	7	31	12	6	8	35	91	30	1395	134	29	226	37
		06-3	16	32	3	15	3	5	0	4	5	2	69	8	1	11	2
BALKAYA	4	A-2	26	48	9	54	22	18	11	51	110	34	1672	136	25	178	30
		C-2	220	424	81	467	197	73	98	478	935	282	13351	1061	190	1390	228
		D-1	292	558	110	616	259	92	122	608	1161	344	14290	1302	227	1670	268
		G-2	20	32	8	47	26	15	12	61	120	36	1824	145	25	188	32
		H-1	93	161	33	187	74	35	37	190	358	112	5595	437	81	568	97
		H-2	57	100	21	123	53	26	28	136	257	81	3999	308	56	410	66
		H-4	263	497	98	556	234	85	114	555	1060	318	13573	1213	213	1570	250
		H-6	330	628	124	684	284	101	132	651	1250	364	15263	1396	244	1776	282
		I-2	140	292	58	338	149	54	64	323	608	179	8087	655	117	837	134
		J-2	146	281	55	311	131	50	60	288	558	168	7805	636	111	811	136

Table S6. Stable (O and C) isotope data of the carbonate samples (‰). $\delta^{18}O_W$ (fluid) computed for 29°C and 44°C.

site	location	sample	$\delta^{13}C$ (VPDB)	$\delta^{18}O$ (VPDB)	$\delta^{18}O$ (VSMOW)	$\delta^{18}O_W$ (29 ºC) (VSMOW)	$\delta^{18}O_W$ (44 ºC) (VSMOW)
SARIHIDIR	1	01	10,7	-12,0	18,5	-11,7	-8,5
		02	8,9	-16,0	14,5	-15,8	-12,6
		03	8,7	-15,0	15,5	-14,7	-11,6
		04	8,7	-16,2	14,3	-16,0	-12,9
		05	11,1	-12,1	18,4	-11,8	-8,6
	2	06-1	9,3	-13,4	17,1	-13,1	-10,0
		06-2	10,9	-11,6	18,9	-11,2	-8,1
		06-3	9,5	-13,2	17,3	-12,9	-9,8
BALKAYA	3	11A	12,2	-9,8	20,7	-9,4	-6,3
		11B	12,1	-9,5	21,0	-9,1	-5,9
		12C	12,2	-10,1	20,4	-9,7	-6,6
		12D	12,1	-10,0	20,5	-9,6	-6,5
	4	A-1	13,2	-9,7	20,8	-9,3	-6,2
		A-2	12,8	-9,8	20,7	-9,4	-6,3
		B	12,7	-9,9	20,6	-9,5	-6,4
		C-1	13,2	-9,6	20,9	-9,2	-6,0
		C-2	13,2	-9,7	20,8	-9,3	-6,2
		D-1	12,9	-9,6	20,9	-9,2	-6,0
		D-2	12,9	-10,1	20,4	-9,7	-6,6
		E--1	12,6	-10,8	19,7	-10,4	-7,3
		E--2	12,7	-10,7	19,8	-10,3	-7,2
		F	11,8	-11,2	19,3	-10,8	-7,7
		G-1	12,6	-11,3	19,2	-10,9	-7,8
		G-2	12,4	-11,2	19,3	-10,8	-7,7
		G-3	11,5	-11,6	18,9	-11,2	-8,1
		H-1	13,0	-10,2	20,3	-9,8	-6,7
		H-2	13,0	-10,3	20,2	-9,9	-6,8
		H-3	13,0	-10,1	20,4	-9,7	-6,6
		H-4	13,1	-10,4	20,1	-10,0	-6,9
		H-5	13,0	-10,5	20,0	-10,1	-7,0
		H-6	12,9	-10,7	19,8	-10,3	-7,2
		H-7	13,0	-10,6	19,9	-10,2	-7,1
		I-1	13,1	-10,1	20,4	-9,7	-6,6
		I-2	13,0	-9,7	20,8	-9,3	-6,2
		J-1	12,9	-10,0	20,5	-9,6	-6,5
		J-2	12,7	-10,1	20,4	-9,7	-6,6